Unusually Strong Long-range Electronic Coupling Across Redox-Active Bridges in M^{3+}/M^{4+} Mixed-Valence Complexes of Group 4 Congeners

Colby Seth Bell,[a] Nathan J. DeYonker,[a] Curtis E. Moore,[b] and Kensha Marie Clark*[a]

[a]Department of Chemistry, University of Memphis, 3744 Walker Ave, Memphis, TN, USA, 38152

[b]Department of Chemistry and Biochemistry, The Ohio State University, 151 W. Woodruff Avenue, Columbus, OH 43210, USA

KEYWORDS (Word Style "BG_Keywords"). If you are submitting your paper to a journal that requires keywords, provide significant keywords to aid the reader in literature retrieval.

ABSTRACT: Homobimetallic complexes of Group 4 metals, supported by the redox-active tetrakis(imino)pyracene (TIP) ligand were synthesized and isolated. The formation of these complexes resulted in LUMOs having significantly lower energies than the free ligand and the respective metal salts, MCl_4 (M = Ti, Zr, Hf), whereby all three complexes were readily reduced by one electron using the mild reductant, Cp^*_2Fe (E^0 = -0.59 V). Spectroscopic characterization and quantum chemical analyses of the reduced species revealed that the resulting complexes are delocalized, borderline Class II-III (Ti) and Class III (Zr, Hf) mixed valence complexes. All three complexes display surprisingly strong long-range electronic coupling between the metal centers, as M to M distances, r_{AB}, are nearly 12 Å. The coupling strengths of Zr and Hf were significantly stronger than those observed for the Ti complex, suggesting that better orbital overlap between the ligand and 4*d* or 5*d* metal centers helps to relieve the instability of the 3+ oxidation state via delocalization.

INTRODUCTION

Multimetallic complexes, or complexes in which metal ions are bridged by ligands having multiple coordination sites, are species that have garnered widespread interest owing to their applications, which range from molecular electronics[1-6] and photovoltaics[7-9] to catalysis[10-17] and biomimetics.[18-21] One area of intense research activity has been the development of molecular wires,[1-2, 7, 22-24] or molecules that facilitate electron transfer and can ultimately be used for charge separation and transfer[25-28] or as building blocks for molecular devices.[29-30] Overwhelmingly, inorganic/organic hybrid species developed as molecular wires feature so-called redox-active ligands as the bridging species.[5, 31-35] This trend is likely due to noninnocence displayed by these systems, whereby admixing of the ligand frontier orbitals and *d*-orbitals of the coordinated metal ion yield the requisite electronic delocalization for wire-like behavior,[36-42] and electronic cooperativity between the metal and ligand can provide additional stability during electron transfer.[43-47] The ligands of choice for these systems largely feature endocyclic imine moieties, such as pyrazine,[5, 48-51] pyridine,[22, 25-26, 52-56] and porphyrin functionalities.[37, 57-61]

It is well established that bidentate exocyclic imines, such as α-diimine ligands, display electronic delocalization when coordinated to various metal centers.[62-69] Furthermore, the electronic properties of exocyclic imines can be easily tuned by varying the substituents on the imine via condensation of the parent ketone with an amine equipped with the desired substituents.[68, 70-71] Considering both the electronic behavior and tunability of this imine ligand class, it is quite surprising that there has been little progress towards the development of bridges based on their framework. One α-diimine framework that holds particular promise as a scaffold for a bridging ligand is bis(arylimino)acenaphtylene (BIAN).[72-73] Structurally, this system consists of a diazabutadiene coordination site that is protected by a naphthylene backbone. Electronically, it can act as a reservoir, whereby electrons can be transferred with ease between the ligand and the central atom.[74-79] For example, in complexes with early transition metals, this ligand system has displayed electronic properties such as delocalization,[80-81] intramolecular electron transfer,[82] and valence tautomerism.[80] The bifunctional BIAN derivative, tetrakis(imino)pyracene (TIP), has been developed by Cowley and coworkers;[83] and similar to its parent, electron transfer between the ligand and a central atom has been observed.[83-87] These results are significant with respect to the potential of this ligand system as a framework for molecular wires.

Bearing in mind the electronic behavior of early transition metal BIAN complexes, we became interested in exploring if these properties could be extended to early transition metal-TIP based molecular wires. As a starting point, we decided to interrogate how changes to the metal center perturb orbital overlap with the ligand, and to parse how these perturbations affect changes to molecular orbital energies of potential monomer units. Limiting our initial study to Group 4 congeners, we synthesized and characterized homobimetallic complexes $Cl_4M(TIP)MCl_4$ (where M = Ti (**1**), Zr (**2**), or Hf(**3**), supported by the tetrakis(3,5-dimethylphenylimino)pyracene (TIP^{Me}) ligand.

Scheme 1. Syntheses of homobimetallic complexes **1**-**3** and their 1-electron reductions to **1**$^{-}$-**3**$^{-}$.

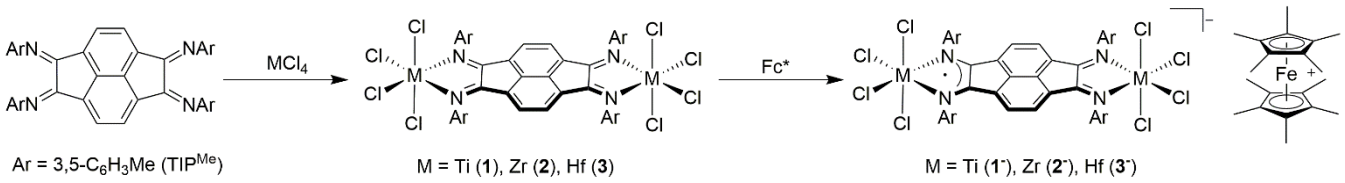

RESULTS AND DISCUSSION

Complexes **1**-**3** were easily prepared in good yields by treating a solution of TIP^{Me} in dichloromethane with two molar equivalents of the respective Group 4 salt, MCl_4 (Scheme 1). Their compositions were confirmed by elemental analysis. Density functional theory (DFT) and time-dependent DFT (TDDFT) computations[88-90] were performed using B3LYP/6-311+G(d,p)/LANL2DZ[91-95] levels of theory with the continuum polarizable cavity model (CPCM).[96-97] See supporting information for full methodological details.

Single crystals of **1**, suitable for X-ray diffraction studies were precipitated by layering a saturated CH_2Cl_2 solution with pentane. For the zirconium and hafnium analogues, **2** and **3**, single crystals were isolated from saturated CH_2Cl_2 solutions by cooling to -34°C or slow evaporation. Selected metrical parameters for these complexes are highlighted in Table 1. The asymmetric units of complexes **1** and **2** are comprised of two independent half molecules which lie on inversion centers (Figure 1). Complex **3** possesses two-fold, crystallographically imposed symmetry, whereby, similar to the asymmetric units of **1** and **2**, the half molecule lies on an inversion center (Figure 1). The molecular structures of **1**-**3** confirm the expected local symmetry, with octahedral geometry about each metal center. Computationally, complexes **1**-**3** possess C_i molecular point group symmetry.

The average N−M−N bite angle of the M−N−C−C−N chelate rings are 73°, 70°, and 71° for complexes **1**, **2**, and **3**, respectively, with the zirconium metal center having the smallest bite angle. These small, ligand-enforced bite angles are consistent with those observed for transition metal complexes supported by neutral BIAN ligands, which typically have N−M−N bite angles in the range of ~70-80°, and contribute significantly to the distortion from idealized octahedral geometry.[98-99] The two apical chloride ligands, Cl(3) and Cl(4) are bent nearly 20° towards the TIP^{Me} ligand, deviating significantly from the expected linearity, and results in surprisingly small Cl(3)−M−Cl(4) bond angles. Complex **2** has the smallest Cl(3)−M−Cl(4) angle (162°), whilst those observed in **1** and **3** are approximately the same (163°). This bending may arise to minimize repulsive interactions from Cl(1) and Cl(2) that lie *trans* to the TIP^{Me} ligand. Similar to their BIAN counterparts, the M−Cl bond lengths of these equatorial chlorides are markedly short relative to their apical counterparts.[98]

Long M−N bond lengths, consistent with the neutral imine form of the ligand, are observed for **1**-**3**.[72, 81-82, 98, 100] Additionally, diagnostic C=N and C−C bond lengths of the TIP^{Me} N−C−C−N chelate, which average 1.28 Å and 1.51 Å, respectively, indicate the neutral form of the ligand, as expected.[72, 101] Both the titanium and zirconium metal centers, in **1** and **2**, can be considered coplanar with the TIP ligand. The molecular structure of **3**, on the contrary, reveals a deviation from planarity, whereby the hafnium metal centers are puckered ~0.57 Å out of the ligand plane, bending towards the ligand in a *prone* fashion.[82, 102-103] This trend was also confirmed computationally. This may be indicative of interactions between hafnium and the π-electrons of the C=N bonds. Most bond lengths computed with DFT are within 0.01 Å of the X-ray crystal structure values (Table SI1). Notably, the computed Zr-Cl bond lengths of **2** are 0.07 – 0.08 Å longer than the experimental values.

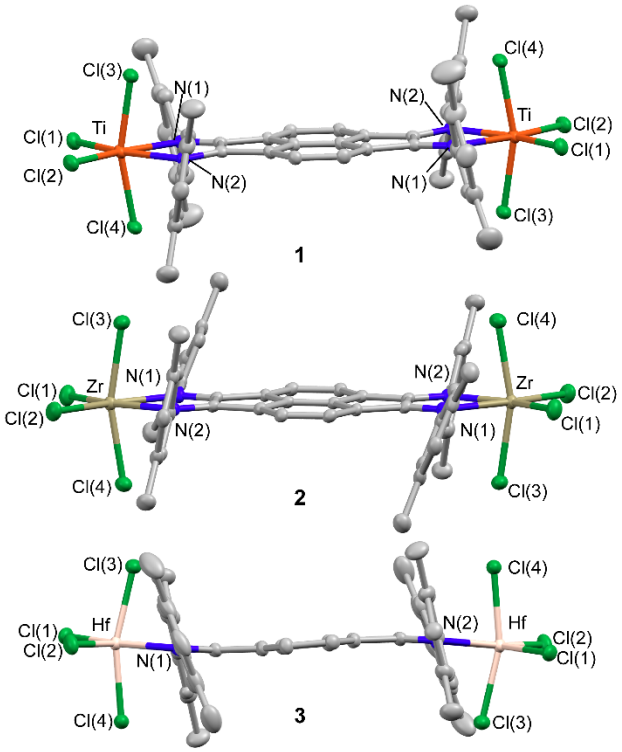

Figure 1. Thermal ellipsoid plots of **1**-**3** as determined by single crystal X-ray diffraction studies. Thermal ellipsoids are shown at 50% probability. Hydrogen atoms and solvent molecules have been omitted for clarity. For complexes **1** and **2** one of two independent molecules are shown. Differences between the two molecules that comprise the unit cell are not significant.

Electronic spectra were collected for dichloromethane solutions of complexes **1**-**3** (Figure SI1) and modeled using TD-DFT (Figure SI2). All three complexes (from experimental and theory) display nearly identical spectra in the range of 200-800 nm. Transitions observed in the visible region are consistent with intraligand (IL) bands, which likely arise from ligand π-π* transitions. The spectra of **1**-**3** are dominated by an intense ligand to metal charge transfer (LMCT) transition, having extinction coefficients of 47,000 (246 nm), 83,000 (244 nm), and 87,000 $M^{-1}cm^{-1}$ (244 nm), respectively. These transitions can be visualized as the combination of several types of electron transfer processes. For example, a charge transfer from a non-bonding orbital of nitrogen to the metal center (n→π*) may occur. Both experimentally determined extinction coefficients and computationally derived relative absorbances for the complexes indicate that complexes **2** and **3**

possess better orbital overlap with the TIP^{Me} ligand their titanium counterpart.

Table 1. Selected bond lengths [Å] for complexes **1**-**3**.

	1	**2**	**3**
M–N(1)	2.234(2)	2.360(3)	2.365(2)
M–N(2)	2.236(2)	2.388(3)	2.333(2)
N(1)–C(1)	1.284(3)	1.279(4)	1.279(3)
N(2)–C(2)	1.279(3)	1.276(4)	1.278(3)
C(1)–C(2)	1.508(3)	1.524(4)	1.519(3)
M–Cl(1)	2.2142(8)	2.3683(6)	2.3462(10)
M–Cl(3)	2.2936(8)	2.3994(6)	2.4185(9)

Electrochemical analysis by cyclic voltammetry (CV), was performed on all three complexes in DCM and THF (Table 2). The voltammograms revealed several reversible redox processes. For complex **1** in particular, many very closely coupled reductions were observed. To better resolve these processes, differential pulse voltammetry (DPV) experiments were conducted. Within the solvent window, multiple reversible and irreversible processes were observed for all complexes. Notably, the first reversible 1-electron reduction of complexes **1**-**3** were reversible and occurred at -0.32 V, -0.53 V, and -0.51 V versus the Fc^{+}/Fc^{0} couple, respectively (Figure 2). These potentials are significantly more positive than those of uncoordinated TIP^{Me} (-1.68 V), Zr^{4+}, and Hf^{4+}, indicating that there are strong interactions between the ligand and metal centers.[104] Moreover, the potentials of the Hf^{4+} and Zr^{4+} complexes are inverted, meaning that the LUMO of **2** is slightly higher in energy than **3**. Though the energy eigenvalues of unoccupied Kohn-Sham orbitals are a qualitative metric at best, computations support the observed trend, with the LUMO energies ranking **2** > **1** ≈ **3** (Table SI2). This behavior supports the likelihood of interactions between hafnium and the ligand C=N bonds as inferred from the XRD data.

It should also be highlighted that in addition to the second reversible reduction observed for **2** and **3** (-0.84 V and -0.86 V, respectively), both complexes have a third reversible reduction (-1.66 V and -1.70 V) that overlaps with the 1-electron reduction of the free TIP^{Me} ligand. The observation of this overlap illustrates that they are *not* purely ligand-based processes: the orbitals associated with the first two reductions of **2** and **3** have must have significant contributions from the metal centers. The electrochemical behavior of the titanium analogue, **1**, differs significantly from **2** and **3**, in that more electrochemical processes were recorded within the solvent window and these processes were all closely coupled with each other. The observed processes, for all three complexes, are Nerstian. This behavior allows the results to be framed in the context of the degree of electronic delocalization between the metal centers.[105] The magnitude of the $\Delta E_{1/2}$ separation between two redox processes signifies the strength of interaction between the two metal sites for homobimetallic systems.[30, 106-108] Larger values of $\Delta E_{1/2}$ are indicative of better stabilization of the mixed-valence complex, which is characteristic of delocalized or Robin and Day Class III mixed-valence complexes.[30, 109-110] By contrast, when $\Delta E_{1/2}$ is very small or close to zero, the bridged metal centers can be considered to be non-interacting (Class I). The value of $\Delta E_{1/2}$ of the first two reductions was found to be 140 mV, 300 mV, and 350 mV for **1**, **2**, and **3**, respectively (Table 2).

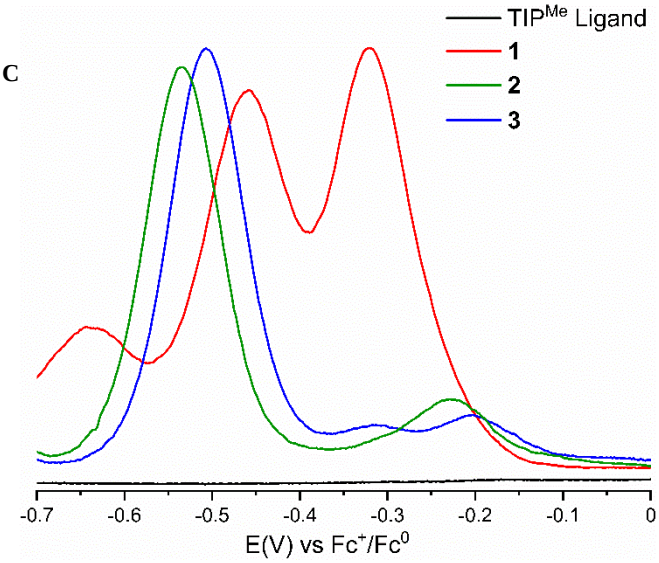

Figure 2. Differential pulse voltammograms of complexes **1**-**3** and TIP^{Me} recorded in DCM (0.10 M [n-Bu_4N][PF_6]) and shown in the range of -0.70-0.00 V vs Fc^{+}/Fc^{0} to highlight $E_{p,1}$. The full voltammograms are included in the supporting information.

Using the values of $\Delta E_{1/2}$, the comproportionation constants, K_{c1} and K_{c2}, were determined for the one- and two-electron reduced derivatives of TIP^{Me} and complexes **1**-**3**. For all three complexes, the values obtained for K_{c1} are larger than expected for complexes of this length, meaning they each have some degree of delocalization;[35, 111-114] however, the value for complex **1**, was several orders of magnitude smaller than those of **2** and **3**. This difference indicates that that reduced derivatives of the titanium complex will be significantly less delocalized in comparison to their zirconium and hafnium counterparts.[115] Furthermore, the values of K_c also suggest that the reduction of **1** yields products that are less delocalized than an uncoordinated TIP^{Me} ligand that has been reduced by one electron. Interestingly, the values of K_{c2} for **2** and **3** increase by more than seven orders of magnitude, suggesting that the two-electron reduced zirconium and hafnium complexes should be more delocalized.

Overall, electrochemical analysis predicts that electronic delocalization should increase as the metal center changes from 3*d* to 5*d* metal ions. This trend is rationalized by considering the stability of the 3+ oxidation state and the degree of orbital overlap between the ligand and the metal ion. Titanium is quite stable as Ti^{3+},[116] whereby the $Ti^{4+/3+}$ couple of independent titanium ions occurs at a significantly lower potential than that of the free ligand.[116-117] On the other hand, the $Zr^{4+/3+}$ and $Hf^{4+/3+}$ redox couples occur at very similar potentials to the $TIP^{0/-1}$ (typically observed between -1.70 V and -2.12 V) and consequently, they are extremely rare.[118-123] This suggests that titanium is more energetically mismatched with the ligand, and upon reduction it may be more favorable for the electron to sit at the metal rather than travel across the higher energy bridge. The energetic similarity of the respective 4*d* and 5*d*

Table 2. Results of Electrochemical Analyses of **1**-**3** performed in CH_2Cl_2 (DCM).

Complex	$E_{p,1}$ (0/-1)[a]	$E_{p,2}$ (-1/-2)[a]	$E_{p,3}$ (-2/-3)[a]	$\Delta E_{1/2}$[b,c]	log K_c (-1)	$\Delta E_{1/2}$[b,c]	log K_c (-2)
TIP^{Me}	-1.68	-2.00	-2.24	320	5.4	240	4.1
1	-0.32	-0.46	-0.63	140	2.3	180	3.1
2	-0.53	-0.84	-1.66	300	5.1	840	14.2
3	-0.51	-0.86	-1.70	350	5.9	840	14.2

[a] V versus Fc^+/Fc^0. [b] Determined using $\Delta E_{1/2} = \Delta E_p$ when $\Delta E_{1/2} > 160\ mV$ and $E_{1/2} = E_p + \frac{\Delta E}{2}$, where ΔE is the pulse amplitude.[124-125] [c]mV.

ions with TIP^{Me} results in better orbital overlap and consequently, increased delocalization is observed.[126]

Encouraged by these results, solutions of **1**-**3** in dichloromethane were treated with the mild reductant, decamethylferrocene (E^0 = -0.59 V in DCM),[127] to yield the 1-electron reduced anionic complexes, **1**$^-$-**3**$^-$ (Scheme 1). The compositions of all three complexes were confirmed by elemental analyses. These reductions were also monitored by UV-Vis spectroscopy, whereby solutions of the starting complexes were titrated with Fc* (Figure 3). Isobestic points were observed at 440 nm; 538, 368, and 331 nm; and 543, 370, and 327 nm for the titrations of **1**, **2**, and **3**, respectively, providing a clear indication that no secondary reactions occur during these reductions.[128-130] Attempts to precipitate X-ray quality single crystals were unsuccessful, as the material appears to decompose after several days in solution to yield unusual MCl_5^- anions (where M = Ti, Zr, or Hf) (Figure SI3).[131-132] We were able, however, to spectroscopically characterize freshly isolated complexes.

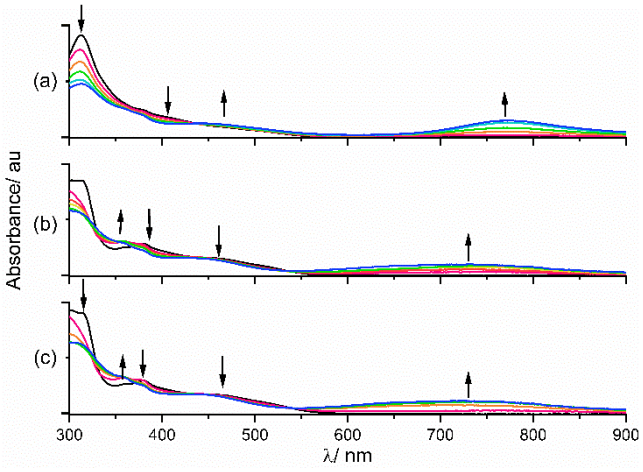

Figure 3. Titration of complexes (a) **1**, (b) **2**, and (c) **3** by Fc* monitored by UV-Vis spectroscopy in the range of 300-900 nm.

The X-band EPR spectra of **1**$^-$-**3**$^-$ were nearly identical, revealing surprising seven-line hyperfine splitting patterns for each complex. Simulations were performed to better understand the origin of these spectral features. The best-fit simulations for all three spectra are centered at $g \approx 2.004$ (Figure 4), which indicate that there is very little spin-orbit coupling to the metal centers in each complex. The isotropic signal suggests that the electron is in a symmetric environment; however, the hyperfine splitting pattern that arises is consistent with asymmetric coupling to the four ligand ^{14}N nuclei and the respective metal nuclei. The likely explanation for these seemingly contradictory characteristics is the *alternating-linewidth effect*.[133-135] The asymmetry observed for the ^{14}N coupling arises from breaking the π-conjugation at one of the M−N−C−C−N chelate rings upon reduction, which alters the coupling at the C−N versus the C═N nitrogen nuclei. These spectra indicate that the arrangement of these bonds is rapidly interchanging due to electron transfer between the metal sites, resulting in out-of-phase modulation of the hyperfine splittings.[133] Consistent with this phenomenon, as the samples were cooled to 77 K, apparent axial signals are visible and the hyperfine splittings are no longer resolved (Figures SI3-SI5).[106, 133, 136-137] The g-values determined for **1**$^-$ at this temperature indicate the electron becomes localized on titanium. On the other hand, the analogous values for **2**$^-$ and **3**$^-$ suggest the electron is still interacting with both the ligand and the metal centers. These features of the spectra are in alignment with the delocalization predicted by the electrochemistry, whereby the 1-electron reduction yields the M^{3+}/M^{4+} mixed-valence complexes. This delocalization was investigated more closely using NIR spectroscopy.

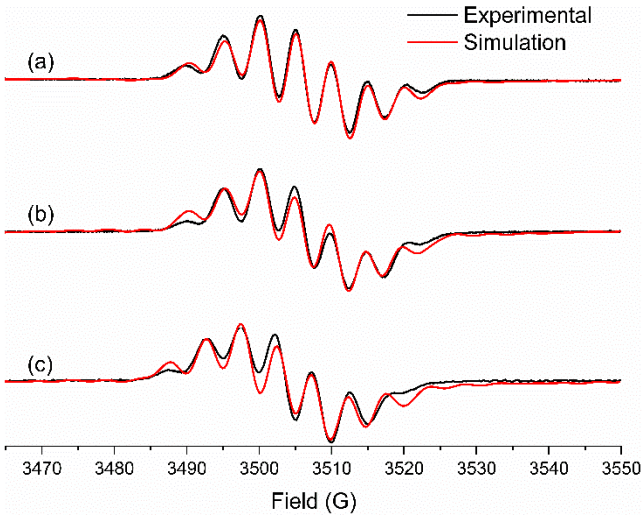

Figure 4. X-band (9.83 GHz) EPR spectra and their best fit simulations: (a) **1**$^-$ (g = 2.004, A(^{14}N) = 4.3 G, A(^{14}N) = 4.3 G, A(^{14}N) = 4.3 G, A(^{14}N) = 0.7 G, A(Ti) = 43 G, A(Ti) = 49 G); (b) **2**$^-$ (g = 2.004, A(^{14}N) = 5.0 G, A(^{14}N) = 5.0 G, A(^{14}N) = 3.9 G, A(^{14}N) = 1.0 G, A(Zr) = 39 G A(Zr) = 39 G); and (c) **3**$^-$ g = 2.004, A(^{14}N) = 5.0 G, A(^{14}N) = 5.0 G, A(^{14}N) = 3.9 G, A(^{14}N) = 1.0 G, A(Hf) = 39 G, A(Hf) = 39 G) in DCM at 298 K.

In the near-IR region (900-2500 nm), broad charge transfer bands were observed for all three complexes (Figure 5). TD-DFT was used to aid in the intervalence charge transfer (IVCT) bands.[138, 139] These bands were found to occur at 1222 nm (8180 cm^{-1}), 1222 nm (8183 cm^{-1}), and 1076 nm (9290 cm^{-1}) for **1**$^-$-**3**$^-$, respectively. The presence of these transitions in

Table 3. Analyses of the IVCT bands for complexes **1**$^{-}$-**3**$^{-}$.

Complex	ν_{max}[a]	$\Delta\nu_{1/2}^{\circ}$[a,b]	$\Delta\nu_{1/2}$[a]	Γ[c]	ϵ_{max}[d]	r_{AB}[e]	H_{AB}[a,f]	H_{AB}[f,g]
1^{-}	8180	4347	2180	0.49	2200	11.565	424	0.053
2^{-}	8183	4350	920	0.78	4900	11.773	4067	0.507
3^{-}	9290	4632	1414	0.70	3700	11.706	4645	0.580

[a] cm^{-1}. [b] $\Delta\nu_{1/2}^{\circ} = (2310 \times \nu_{max})^{1/2}$ at 298 K. [c] If $\Gamma = 0$ a system can be categorized as Class II; if $0 < \Gamma < 0.5$, a system can be categorized as borderline Class II-III; and if $0.5 \leq \Gamma$, a system can be categorized as Class III. [d] $M^{-1}\ cm^{-1}$. [e] Estimated metal to metal distance in Å. [f] For borderline Class II-III, $H_{AB} = 2.06 \times 10^{-2}(\nu_{max}\epsilon_{max}\Delta\nu_{1/2})^{1/2}/r_{AB}$; for Class III, $H_{AB} = \nu_{max}/2$. [g] eV.

this region provide further confirmation of mixed-valency and delocalization.[140-142] Notably, IVCT transitions in this region are characteristic of Class II or Class III mixed-valence complexes, whereby the system is valence trapped (i.e. the redox sites are not energetically identical, but the energetic barrier to for electron transfer is small) or of delocalized valency (i.e. the two metal sites are non-discrete; there is virtually no barrier for electron transfer).[115] The IVCT bands of these complexes appear to have a low-energy cutoff that is characteristic of borderline Class II-III and Class III species. By applying Hush's theory for symmetrical charge-transfer complexes,[143-144] it was determined that the respective theoretical bandwidths at half-intensity, $\Delta\nu_{1/2}^{\circ}$, for the three complexes are broader than the experimentally determined values, $\Delta\nu_{1/2}$ (Table 2). This difference confirms that there is electronic delocalization between the two metal centers in **1**$^{-}$-**3**$^{-}$. The degree of delocalization was measured using the parameter, Γ,[145] defined as (equation 1),

$$\Gamma = 1 - \frac{\Delta\nu_{1/2}}{\Delta\nu_{1/2}^{\circ}} \qquad (1)$$

Based on the determined values of Γ (Table 3), **1**$^{-}$ can be considered borderline Class II-III, whilst complexes **2**$^{-}$ and **3**$^{-}$ can be squarely categorized as Robin and Day Class III mixed-valence complexes, whereby the two metal redox sites in each complex are virtually indistinguishable.[110] The degree of delocalization predicted by Γ is consistent with the expected behavior derived from $\Delta E_{1/2}$ values obtained in our electrochemical experiments. Molecular orbital contour plots of frontier orbitals validate differences in the electronic delocalization/coupling behavior of the reduced complexes. In Figure 6, the HOMO and LUMO of **1**$^{-}$-**3**$^{-}$ are symmetric and display delocalized character. The NIR data was also used to determine the estimated electronic couplings between the two metal sites, H_{AB}, which were determined to be 424, 4092, and 4645 cm^{-1}, for **1**$^{-}$-**3**$^{-}$, respectively (Table 3). These values indicate that coupling between metal sites is strong at relatively long distances (~12 Å), suggesting electron transfer proceeds by way of through-bond electronic coupling.[23, 60, 146-149]

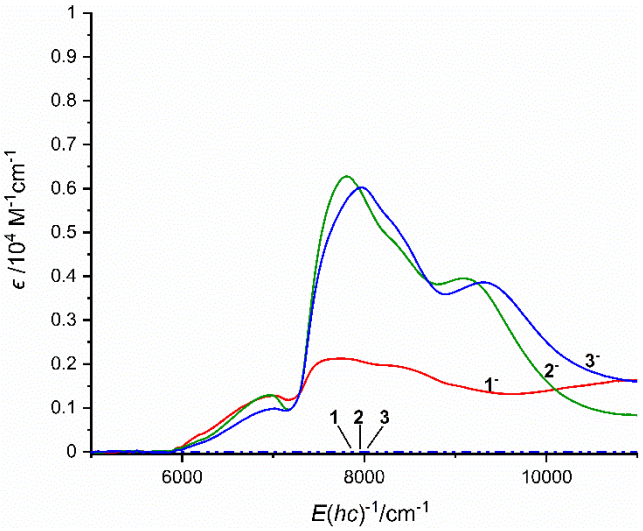

Figure 5. NIR spectra (5000-11,000 cm^{-1}) of complexes **1**-**3** and reduced **1**$^{-}$-**3**$^{-}$ collected in DCM at 298 K.

CONCLUSIONS

In conclusion, coordination of the TIP ligand to Group 4 transition metal centers results in significant orbital overlap which yield, upon reduction, delocalized M^{3+}/M^{4+} mixed valence complexes. The combination of the stability of Ti^{3+} and lower orbital overlap of the 3*d* metal ion, results in less delocalization for the titanium complex in comparison to zirconium and hafnium, for which the instability of the Zr^{3+} and Hf^{3+} oxidation states are relieved by distributing the electron between the two metal sites. Nevertheless, all three systems demonstrate extremely strong long-range electronic coupling that is consistent with through bond coupling. Group 4 transition metal complexes, in particular zirconium and hafnium, are oft overlooked when designing electronic materials because of their preference for a d^0 electron configuration. The systems described in this work demonstrate that by using metal centers with unstable oxidation states, in conjunction with an energetically appropriate ligand, electronic delocalization and communication between metal sites can be facilitated. This principle will be applied strategically for the development of new electronic materials and catalysts.

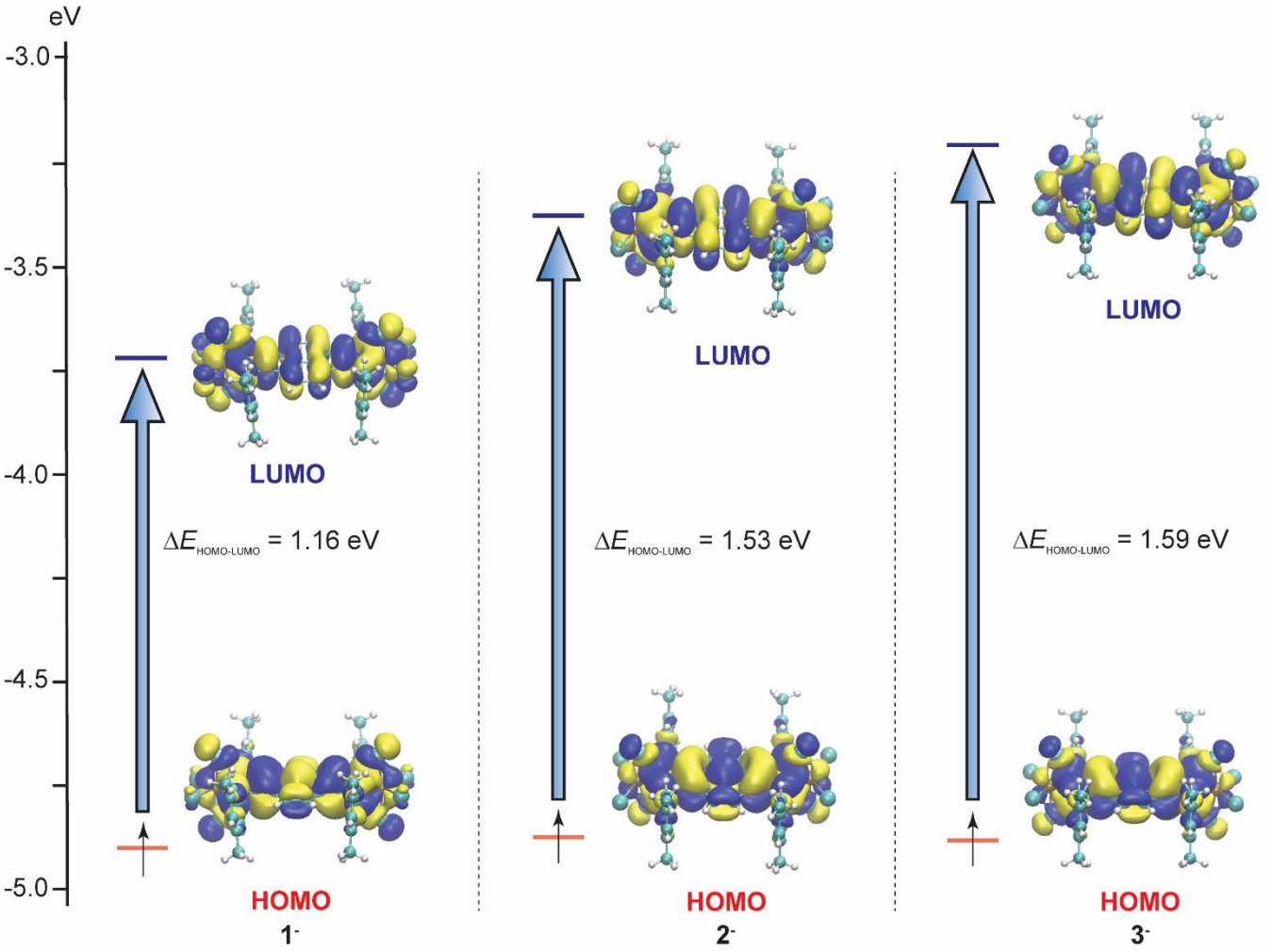

Figure 6. Molecular orbital diagrams for **1**$^{-}$, **2**$^{-}$, and **3**$^{-}$ from DFT calculations. The isovalues of the contour plots were set at ±0.01.

ASSOCIATED CONTENT

Supporting Information

The Supporting information is available free of charge via the Internet at http://pubs.acs.org."

Full details of experimental procedures, NMR, EPR, UV-Vis, NIR spectra, voltammograms, computational results, all computed Cartesian coordinates, and crystallographic details.

Crystallographic information files for **1**, **2**, and **3**.

AUTHOR INFORMATION

Corresponding Author

* (K.M.C.) E-mail: kensha.clark@memphis.edu

Author Contributions

The manuscript was written through contributions of all authors. / All authors have given approval to the final version of the manuscript.

Funding Sources

ACS-PRF 60364DNI3 (K.M.C.)

NSF CAREER BIO-1846408 (N.J.D.Y.)

ACKNOWLEDGMENT

K.M.C thanks Prof. Michael Shaw (Southern Illinois University Edwardsville) for advice regarding DPV experiments. K.M.C. also thanks Prof. Brad S. Pierce (University of Alabama) and Dr. Molly Lockart (University of Alabama) for use of the UA EPR Laboratory.

REFERENCES

1. Ward, M. D., Metal-Metal Interactions in Binuclear Complexes Exhibiting Mixed-Valency - Molecular Wires and Switches. *Chem. Soc. Rev.* **1995,** *24* (2), 121-134.
2. Tanaka, Y.; Kiguchi, M.; Akita, M., Inorganic and Organometallic Molecular Wires for Single-Molecule Devices. *Chem. Eur. J.* **2017,** *23* (20), 4740-4740.
3. Naher, M.; Roemer, M.; Koutsantonis, G. A.; Low, P. J., Metal Complexes for Molecular Electronics. In *Reference Module in Chemistry, Molecular Sciences and Chemical Engineering*, 2020.
4. Dei, A.; Gatteschi, D.; Sangregorio, C.; Sorace, L., Quinonoid metal complexes: Toward molecular switches. *Acc. Chem. Res.* **2004,** *37* (11), 827-835.
5. Perlepe, P.; Oyarzabal, I.; Pedersen, K. S.; Negrier, P.; Mondieig, D.; Rouzieres, M.; Hillard, E. A.; Wilhelm, F.; Rogalev, A.; Suturina, E. A.; Mathoniere, C.; Clerac, R., $Cr(pyrazine)_2(OSO_2CH_3)_2$: A two-dimensional coordination polymer with an antiferromagnetic ground state. *Polyhedron* **2018,** *153*, 248-253.
6. Kawamura, A.; Filatov, A. S.; Anderson, J. S.; Jeon, I.-R., Slow Magnetic Relaxation of Co(II) Single Chains

Embedded within Metal–Organic Superstructures. *Inorg. Chem.* **2019,** *58* (6), 3764-3773.
7. Gilbert, M.; Albinsson, B., Photoinduced charge and energy transfer in molecular wires. *Chem. Soc. Rev.***2015,** *44* (4), 845-862.
8. Jena, A. K.; Kulkarni, A.; Miyasaka, T., Halide Perovskite Photovoltaics: Background, Status, and Future Prospects. *Chem. Rev.* **2019,** *119* (5), 3036-3103.
9. Shyni, R.; Biju, S.; Reddy, M. L. P.; Cowley, A. H.; Findlater, M., Synthesis, Crystal Structures, and Photophysical Properties of Homodinuclear Lanthanide Xanthene-9-carboxylates. *Inorg. Chem.* **2007,** *46* (26), 11025-11030.
10. Wurster, B.; Grumelli, D.; Hotger, D.; Gutzler, R.; Kern, K., Driving the Oxygen Evolution Reaction by Nonlinear Cooperativity in Bimetallic Coordination Catalysts. *J. Am. Chem. Soc.* **2016,** *138* (11), 3623-3626.
11. Charles, R. M.; Brewster, T. P., H_2 and carbon-heteroatom bond activation mediated by polarized heterobimetallic complexes. *Coord. Chem. Rev.* **2021,** *433*, 213765.
12. Bodio, E.; Picquet, M.; Le Gendre, P., "Early–Late" Heterobimetallic Catalysis and Beyond. In *Homo- and Heterobimetallic Complexes in Catalysis*, 2015; pp 139-186.
13. Shibasaki, M.; Kanai, M.; Matsunaga, S.; Kumagai, N., Multimetallic Multifunctional Catalysts for Asymmetric Reactions. In *Bifunctional Molecular Catalysis*, 2011; pp 1-30.
14. Singh, D.; Buratto, W. R.; Torres, J. F.; Murray, L. J., Activation of Dinitrogen by Polynuclear Metal Complexes. *Chem. Rev.* **2020,** *120* (12), 5517-5581.
15. Dalle, K. E.; Warnan, J.; Leung, J. J.; Reuillard, B.; Karmel, I. S.; Reisner, E., Electro- and Solar-Driven Fuel Synthesis with First Row Transition Metal Complexes. *Chem. Rev.* **2019,** *119* (4), 2752-2875.
16. Coombs, J.; Perry, D.; Kwon, D.-H.; Thomas, C. M.; Ess, D. H., Why Two Metals Are Better Than One for Heterodinuclear Cobalt–Zirconium-Catalyzed Kumada Coupling. *Organometallics* **2018,** *37* (22), 4195-4203.
17. Gramigna, K. M.; Dickie, D. A.; Foxman, B. M.; Thomas, C. M., Cooperative H_2 Activation across a Metal–Metal Multiple Bond and Hydrogenation Reactions Catalyzed by a Zr/Co Heterobimetallic Complex. *ACS Catal.* **2019,** *9* (4), 3153-3164.
18. Dalle, K. E.; Meyer, F., Modelling Binuclear Metallobiosites: Insights from Pyrazole-Supported Biomimetic and Bioinspired Complexes. *Eur. J. Inorg. Chem.* **2015,** (21), 3391-3405.
19. Thomas, C. M.; Liu, T.; Hall, M. B.; Darensbourg, M. Y., Regioselective $^{12}CO/^{13}CO$ exchange activity of a mixed-valent Fe(II)Fe(I) model of the H_{ox} state of [FeFe]-hydrogenase. *Chem. Commun.* **2008,** (13), 1563-1565.
20. Ghosh, P.; Ding, S.; Chupik, R. B.; Quiroz, M.; Hsieh, C.-H.; Bhuvanesh, N.; Hall, M. B.; Darensbourg, M. Y., A matrix of heterobimetallic complexes for interrogation of hydrogen evolution reaction electrocatalysts. *Chem. Sci.* **2017,** *8* (12), 8291-8300.
21. Liu, T.; Darensbourg, M. Y., A Mixed-Valent, Fe(II)Fe(I), Diiron Complex Reproduces the Unique Rotated State of the [FeFe]Hydrogenase Active Site. *J. Am. Chem. Soc.* **2007,** *129* (22), 7008-7009.
22. Maeda, H.; Sakamoto, R.; Nishihara, H., Rapid Electron Transport Phenomenon in the Bis(terpyridine) Metal Complex Wire: Marcus Theory and Electrochemical Impedance Spectroscopy Study. *J. Phys. Chem. Letters* **2015,** *6* (19), 3821-3826.
23. Ricks, A. B.; Brown, K. E.; Wenninger, M.; Karlen, S. D.; Berlin, Y. A.; Co, D. T.; Wasielewski, M. R., Exponential Distance Dependence of Photoinitiated Stepwise Electron Transfer in Donor-Bridge-Acceptor Molecules: Implications for Wirelike Behavior. *J. Am. Chem. Soc.* **2012,** *134* (10), 4581-4588.
24. Andzane, J.; Prikulis, J.; Dvorsek, D.; Mihailovic, D.; Erts, D., Two-terminal nanoelectromechanical bistable switches based on molybdenum-sulfur-iodine molecular wire bundles. *Nanotechnology* **2010,** *21* (12), 125706.
25. Sakamoto, R.; Katagiri, S.; Maeda, H.; Nishihara, H., Bis(terpyridine) metal complex wires: Excellent long-range electron transfer ability and controllable intrawire redox conduction on silicon electrode. *Coord. Chem. Rev.* **2013,** *257* (9-10), 1493-1506.
26. Sakamoto, R.; Ohirabaru, Y.; Matsuoka, R.; Maeda, H.; Katagiri, S.; Nishihara, H., Orthogonal bis(terpyridine)-Fe(II) metal complex oligomer wires on a tripodal scaffold: rapid electron transport. *Chem. Commun.* **2013,** *49* (64), 7108-7110.
27. Aragones, A. C.; Darwish, N.; Ciampi, S.; Jiang, L.; Roesch, R.; Ruiz, E.; Nijhuis, C. A.; Diez-Perez, I., Control over Near-Ballistic Electron Transport through Formation of Parallel Pathways in a Single-Molecule Wire. *J. Am. Chem. Soc.* **2019,** *141* (1), 240-250.
28. Wiberg, J.; Guo, L. J.; Pettersson, K.; Nilsson, D.; Ljungdahl, T.; Martensson, J.; Albinsson, B., Charge recombination versus charge separation in donor-bridge-acceptor systems. *J. Am. Chem. Soc.* **2007,** *129* (1), 155-163.
29. Harvey, E. C.; Feringa, B. L.; Vos, J. G.; Browne, W. R.; Pryce, M. T., Transition metal functionalized photo- and redox-switchable diarylethene based molecular switches. *Coord. Chem. Rev.* **2015,** *282*, 77-86.
30. Aguirre-Etcheverry, P.; O'Hare, D., Electronic Communication through Unsaturated Hydrocarbon Bridges in Homobimetallic Organometallic Complexes. *Chem. Rev.* **2010,** *110* (8), 4839-4864.
31. Chandra, S.; Weisser, F.; Klenk, S.; Beerhues, J.; Schweinfurth, D.; Sarkar, B., Dinuclear Ru^{II} complexes with quinonoid bridges: tuning the electrochemical and spectroscopic properties of redox-switchable NIR dyes through judicious bridge design. *Dalton Trans.* **2020,** *49* (24), 8354-8366.
32. Rotthowe, N.; Zwicker, J.; Winter, R. F., Influence of Quinoidal Distortion on the Electronic Properties of Oxidized Divinylarylene-Bridged Diruthenium Complexes. *Organometallics* **2019,** *38* (14), 2782-2799.
33. Hassenruck, C.; Mang, A.; Winter, R. F., Mixed-Valent Ruthenocene-Vinylruthenium Conjugates: Valence Delocalization Despite Chemically Different Redox Sites. *Inorg. Chem.* **2019,** *58* (4), 2695-2707.
34. Mondal, D.; Majee, M. C.; Kundu, S.; Mortel, M.; Abbas, G.; Endo, A.; Khusniyarov, M. M.; Chaudhury, M., Dinuclear Iron(III) and Cobalt(III) Complexes Featuring a Biradical Bridge: Their Molecular Structures and Magnetic, Spectroscopic, and Redox Properties. *Inorg. Chem.* **2018,** *57* (3), 1004-1016.
35. Mandal, A.; Hoque, M. A.; Grupp, A.; Paretzki, A.; Kaim, W.; Lahiri, G. K., Analysis of Redox Series of Unsymmetrical 1,4-Diamido-9,10-anthraquinone-Bridged Diruthenium Compounds. *Inorg. Chem.* **2016,** *55* (5), 2146-2156.
36. Ward, M. D.; McCleverty, J. A., Non-innocent behaviour in mononuclear and polynuclear complexes: consequences for redox and electronic spectroscopic properties. *J. Chem. Soc., Dalton Trans.* **2002,** (3), 275-288.
37. Kaim, W., The Shrinking World of Innocent Ligands: Conventional and Non-Conventional Redox-Active Ligands. *Eur. J. Inorg. Chem.* **2012,** (3), 343-348.
38. Kaim, W., Manifestations of Noninnocent Ligand Behavior. *Inorg. Chem.* **2011,** *50* (20), 9752-9765.
39. Gaudette, A. I.; Jeon, I.-R.; Anderson, J. S.; Grandjean, F.; Long, G. J.; Harris, T. D., Electron Hopping through Double-Exchange Coupling in a Mixed-Valence

Diiminobenzoquinone-Bridged Fe_2 Complex. *J. Am. Chem. Soc.* **2015,** *137* (39), 12617-12626.
40. Ziebel, M. E.; Darago, L. E.; Long, J. R., Control of Electronic Structure and Conductivity in Two-Dimensional Metal–Semiquinoid Frameworks of Titanium, Vanadium, and Chromium. *J. Am. Chem. Soc.* **2018,** *140* (8), 3040-3051.
41. Chakarawet, K.; Harris, T. D.; Long, J. R., Semiquinone radical-bridged M_2 (M = Fe, Co, Ni) complexes with strong magnetic exchange giving rise to slow magnetic relaxation. *Chem. Sci.* **2020,** *11* (31), 8196-8203.
42. Frazier, B. A.; Wolczanski, P. T.; Keresztes, I.; DeBeer, S.; Lobkovsky, E. B.; Pierpont, A. W.; Cundari, T. R., Synthetic Approaches to $(smif)_2Ti$ (smif=1,3-di-(2-pyridyl)-2-azaallyl) Reveal Redox Non-Innocence and C-C Bond-Formation. *Inorg. Chem.* **2012,** *51* (15), 8177-8186.
43. Eberle, B.; Damjanović, M.; Enders, M.; Leingang, S.; Pfisterer, J.; Krämer, C.; Hübner, O.; Kaifer, E.; Himmel, H.-J., Radical Monocationic Guanidino-Functionalized Aromatic Compounds (GFAs) as Bridging Ligands in Dinuclear Metal Acetate Complexes: Synthesis, Electronic Structure, and Magnetic Coupling. *Inorg. Chem.* **2016,** *55* (4), 1683-1696.
44. Wiesner, S.; Wagner, A.; Kaifer, E.; Himmel, H.-J., A Valence Tautomeric Dinuclear Copper Tetrakisguanidine Complex. *Chem. Eur. J.* **2016,** *22* (30), 10438-10445.
45. Ziesak, A.; Wesp, T.; Hübner, O.; Kaifer, E.; Wadepohl, H.; Himmel, H.-J., Counter-ligand control of the electronic structure in dinuclear copper-tetrakisguanidine complexes. *Dalton Trans.* **2015,** *44* (44), 19111-19125.
46. Olatunji-Ojo, O. A.; Cundari, T. R., C–H Activation by Multiply Bonded Complexes with Potentially Noninnocent Ligands: A Computational Study. *Inorg. Chem.* **2013,** *52* (14), 8106-8113.
47. Bezpalko, M. W.; Foxman, B. M.; Thomas, C. M., Noninnocent Behavior of Bidentate Amidophosphido $[NP]^{2-}$ Ligands upon Coordination to Copper. *Inorg. Chem.* **2013,** *52* (21), 12329-12331.
48. Creutz, C.; Taube, H., Direct approach to measuring the Franck-Condon barrier to electron transfer between metal ions. *J. Am. Chem. Soc.* **1969,** *91* (14), 3988-3989.
49. Flores-Torres, S.; Hutchison, G. R.; Soltzberg, L. J.; Abruna, H. D., Ruthenium molecular wires with conjugated bridging ligands: Onset of band formation in linear inorganic conjugated oligomers. *J. Am. Chem. Soc.* **2006,** *128* (5), 1513-1522.
50. Pedersen, K. S.; Perlepe, P.; Aubrey, M. L.; Woodruff, D. N.; Reyes-Lillo, S. E.; Reinholdt, A.; Voigt, L.; Li, Z. S.; Borup, K.; Rouzieres, M.; Samohvalov, D.; Wilhelm, F.; Rogalev, A.; Neaton, J. B.; Long, J. R.; Clerac, R., Formation of the layered conductive magnet $CrCl_2(pyrazine)_2$ through redox-active coordination chemistry. *Nature Chemistry* **2018,** *10* (10), 1056-1061.
51. Ito, T.; Hamaguchi, T.; Nagino, H.; Yamaguchi, T.; Kido, H.; Zavarine, I. S.; Richmond, T.; Washington, J.; Kubiak, C. P., Electron transfer on the infrared vibrational time scale in-the mixed valence state of 1,4-pyrazine- and 4,4'-bipyridine-bridged ruthenium cluster complexes. *J. Am. Chem. Soc.* **1999,** *121* (19), 4625-4632.
52. Tom, G. M., Creutz, C., Taube, H.; Mixed valence complexes of ruthenium ammines with 4,4'-bipyridine as bridging ligand. *J. Am. Chem. Soc.* **1974,** *96* (25), 7827-7829.
53. McCleverty, J. A.; Ward, M. D., The role of bridging ligands in controlling electronic and magnetic properties in polynuclear complexes. *Acc. Chem. Res.* **1998,** *31* (12), 842-851.
54. Carlson, C. N.; Scott, B. L.; Martin, R. L.; Thompson, J. D.; Morris, D. E.; John, K. D., Control of electronic and magnetic coupling via bridging ligand geometry in a bimetallic ytterbocene complex. *Inorg. Chem.* **2007,** *46* (12), 5013-5022.
55. Carlson, C. N.; Veauthier, J. M.; John, K. D.; Morris, D. E., Electronic and magnetic properties of bimetallic ytterbocene complexes: The impact of bridging ligand geometry. *Chem. Eur. J.* **2008,** *14* (2), 422-431.
56. Serroni, S.; Juris, A.; Venturi, M.; Campagna, S.; Resino, I. R.; Denti, G.; Credi, A.; Balzani, V., Polynuclear metal complexes of nanometre size. A versatile synthetic strategy leading to luminescent and redox-active dendrimers made of an osmium(II)-based core and ruthenium(II)-based units in the branches. *J. Mater. Chem.* **1997,** *7* (7), 1227-1236.
57. Kocherzhenko, A. A.; Patwardhan, S.; Grozema, F. C.; Anderson, H. L.; Siebbeles, L. D. A., Mechanism of Charge Transport along Zinc Porphyrin-Based Molecular Wires. *J. Am. Chem. Soc.* **2009,** *131* (15), 5522-5529.
58. Blusch, L. K.; Mitevski, O.; Martin-Diaconescu, V.; Propper, K.; DeBeer, S.; Dechert, S.; Meyer, F., Selective Synthesis and Redox Sequence of a Heterobimetallic Nickel/Copper Complex of the Noninnocent Siamese-Twin Porphyrin. *Inorg. Chem.* **2014,** *53* (15), 7876-7885.
59. Dorazio, S. J.; Vogel, A.; Dechert, S.; Nevonen, D. E.; Nemykin, V. N.; Bruckner, C.; Meyer, F., Siamese-Twin Porphyrin Goes Platinum: Group 10 Monometallic, Homobimetallic, and Heterobimetallic Complexes. *Inorg. Chem.* **2020,** *59* (10), 7290-7305.
60. Wang, R.; Ko, C.-H.; Brugh, A. M.; Bai, Y.; Forbes, M. D. E.; Therien, M. J., Topology, Distance, and Orbital Symmetry Effects on Electronic Spin–Spin Couplings in Rigid Molecular Systems: Implications for Long-Distance Spin–Spin Interactions. *The J. Phys. Chem. A* **2020,** *124* (37), 7411-7415.
61. Kilsa, K.; Kajanus, J.; Macpherson, A. N.; Martensson, J.; Albinsson, B., Bridge-dependent electron transfer in porphyrin-based donor-bridge-acceptor systems. *J. Am. Chem. Soc.* **2001,** *123* (13), 3069-3080.
62. de Zwart, F. J.; Reus, B.; Laporte, A. A. H.; Sinha, V.; de Bruin, B., Metrical Oxidation States of 1,4-Diazadiene-Derived Ligands. *Inorg. Chem.* **2021,** *60* (5), 3274-3281.
63. Nishiyama, H.; Ikeda, H.; Saito, T.; Kriegel, B.; Tsurugi, H.; Arnold, J.; Mashima, K., Structural and Electronic Noninnocence of alpha-Diimine Ligands on Niobium for Reductive C-Cl Bond Activation and Catalytic Radical Addition Reactions. *J. Am. Chem. Soc.* **2017,** *139* (18), 6494-6505.
64. Yan, H. H.; Wu, B. T.; Meng, Y. S.; Zhang, W. X.; Xi, Z. F., Synthesis, Structure, and Magnetic Properties of Rare-Earth Bis(diazabutadiene) Diradical Complexes. *Inorg. Chem.* **2021,** *60* (3), 1315-1319.
65. Ghosh, M.; Sproules, S.; Weyhermuller, T.; Wieghardt, K., (alpha-diimine)chromium complexes: Molecular and electronic structures; A combined experimental and density functional theoretical study. *Inorg. Chem.* **2008,** *47* (13), 5963-5970.
66. Khusniyarov, M. M.; Weyhermuller, T.; Bill, E.; Wieghardt, K., Tuning the Oxidation Level, the Spin State, and the Degree of Electron Delocalization in Homo- and Heteroleptic Bis(α-diimine)iron Complexes. *J. Am. Chem. Soc.* **2009,** *131* (3), 1208-1221.
67. Mashima, K., Redox-Active α-Diimine Complexes of Early Transition Metals: From Bonding to Catalysis. *Bull. Chem. Soc. Jpn.* **2020,** *93* (6), 799-820.
68. Wilson, H. H.; Koellner, C. A.; Hannan, Z. M.; Endy, C. B.; Bezpalko, M. W.; Piro, N. A.; Kassel, W. S.; Sonntag, M. D.; Graves, C. R., Synthesis and Characterization of Neutral Ligand alpha-Diirnine Complexes of Aluminum with Tunable Redox Energetics. *Inorg. Chem.* **2018,** *57* (16), 9622-9633.
69. Heins, S. P.; Wolczanski, P. T.; Cundari, T. R.; MacMillan, S. N., Redox non-innocence permits catalytic nitrene

carbonylation by (dadi)Ti═NAd (Ad = adamantyl). *Chem. Sci.* **2017,** *8* (5), 3410-3418.
70. Gasperini, M.; Ragaini, F.; Cenini, S., Synthesis of Ar-BIAN ligands (Ar-BIAN = bis(aryl)acenaphthenequinonediimine) having strong electron-withdrawing substituents on the aryl rings and their relative coordination strength toward palladium(0) and -(II) complexes. *Organometallics* **2002,** *21* (14), 2950-2957.
71. Gasperini, M.; Ragaini, F.; Gazzola, E.; Caselli, A.; Macchi, P., Synthesis of mixed Ar,Ar′-BIAN ligands (Ar,Ar′-BIAN = bis(aryl)acenaphthenequinonediimine). Measurement of the coordination strength of hemilabile ligands with respect to their symmetric counterparts. *Dalton Trans.* **2004,** (20), 3376-3382.
72. Fedushkin, I. L.; Skatova, A. A.; Chudakova, V. A.; Fukin, G. K., Four-step reduction of dpp-bian with sodium metal: Crystal structures of the sodium salts of the mono-, di-, tri- and tetraanions of dpp-bian. *Angew. Chem., Int. Ed.* **2003,** *42* (28), 3294-3298.
73. Hill, N. J.; Vargas-Baca, I.; Cowley, A. H., Recent developments in the coordination chemistry of bis(imino)acenaphthene (BIAN) ligands with *s*- and *p*-block elements. *Dalton Trans.* **2009,** (2), 240-253.
74. Schelter, E. J.; Wu, R.; Scott, B. L.; Thompson, J. D.; Cantat, T.; John, K. D.; Batista, E. R.; Morris, D. E.; Kiplinger, J. L., Actinide Redox-Active Ligand Complexes: Reversible Intramolecular Electron-Transfer in $U(dpp\text{-}BIAN)_2$/$U(dpp\text{-}BIAN)_2(THF)$. *Inorg. Chem.* **2009,** *49* (3), 924-933.
75. Fedushkin, I. L.; Makarov, V. M.; Sokolov, V. G.; Fukin, G. K., Acenaphthene-1,2-diimine chromium complexes. *Dalton Trans* **2009,** (38), 8047-53.
76. Fedushkin, I. L.; Maslova, O. V.; Morozov, A. G.; Dechert, S.; Demeshko, S.; Meyer, F., Genuine Redox Isomerism in a Rare-Earth-Metal Complex. *Angew. Chem., Int. Ed.* **2012,** *51* (42), 10584-10587.
77. Fedushkin, I. L.; Sokolov, V. G.; Piskunov, A. V.; Makarov, V. M.; Baranov, E. V.; Abakumov, G. A., Adaptive behavior of a redox-active gallium carbenoid in complexes with molybdenum. *Chem. Commun.* **2014,** *50* (70), 10108-10111.
78. Larson, P. J.; Wekesa, F. S.; Singh, A.; Smith, C. R.; Rajput, A.; McGovern, G. P.; Unruh, D. K.; Cozzolino, A. F.; Findlater, M., Synthesis, characterization, electrochemical properties and theoretical calculations of (BIAN) iron complexes. *Polyhedron* **2019,** *159*, 365-374.
79. Wekesa, F. S.; Arias-Ugarte, R.; Kong, L.; Sumner, Z.; McGovern, G. P.; Findlater, M., Iron-Catalyzed Hydrosilylation of Aldehydes and Ketones under Solvent-Free Conditions. *Organometallics* **2015,** *34* (20), 5051-5056.
80. Bendix, J.; Clark, K. M., Delocalization and Valence Tautomerism in Vanadium Tris(iminosemiquinone) Complexes. *Angew. Chem., Int. Ed.* **2016,** *55* (8), 2748-2752.
81. Clark, K. M.; Bendix, J.; Heyduk, A. F.; Ziller, J. W., Synthesis and Characterization of a Neutral Titanium Tris(iminosemiquinone) Complex Featuring Redox-Active Ligands. *Inorg. Chem.* **2012,** *51* (14), 7457-7459.
82. Clark, K. M., Synthesis and Reactivity of Low-Coordinate Titanium Synthons Supported by a Reduced Redox-Active Ligand. *Inorg. Chem.* **2016,** *55* (13), 6443-6448.
83. Vasudevan, K. V.; Findlater, M.; Cowley, A. H., Synthesis and reactivity of tetrakis(imino) pyracene (TIP) ligands; bifunctional analogues of the BIAN ligand class. *Chem. Commun.* **2008,** (16), 1918-1919.
84. Vasudevan, K. V.; Cowley, A. H., New bimetallic complexes supported by a tetrakis(imino)pyracene (TIP) ligand. *Nouv. J. Chim.* **2011,** *35* (10), 2043-2046.
85. Vasudevan, K. V.; Findlater, M.; Vargas-Baca, I.; Cowley, A. H., Tetrakis(imino)pyracene Complexes Exhibiting Multielectron Redox Processes. *J. Am. Chem. Soc.* **2012,** *134* (1), 176-178.
86. Vasudevan, K. V.; Vargas-Baca, I.; Cowley, A. H., Naphthalene-Mediated Electronic Communication in Tetrakis(imino)pyracene Complexes. *Angew. Chem., Int. Ed.* **2009,** *48* (44), 8369-8371.
87. Prades, A.; Peris, E.; Alcarazo, M., Pyracenebis(imidazolylidene): A New Janus-Type Biscarbene and Its Coordination to Rhodium and Iridium. *Organometallics* **2012,** *31* (12), 4623-4626.
88. Becke, A. D., Density-functional thermochemistry. III. The role of exact exchange. *J. Chem. Phys.* **1993,** *98* (7), 5648-5652.
89. Furche, F.; Ahlrichs, R., Adiabatic time-dependent density functional methods for excited state properties. *J. Chem. Phys.* **2002,** *117* (16), 7433-7447.
90. Furche, F.; Ahlrichs, R., Erratum: "Time-dependent density functional methods for excited state properties" [J. Chem. Phys. 117, 7433 (2002)]. *J. Chem. Phys.* **2004,** *121* (24).
91. Hay, P. J.; Wadt, W. R., Ab initio effective core potentials for molecular calculations. Potentials for K to Au including the outermost core orbitals. *J. Chem. Phys.* **1985,** *82* (1), 299-310.
92. Hay, P. J.; Wadt, W. R., Ab initio effective core potentials for molecular calculations. Potentials for the transition metal atoms Sc to Hg. *J. Chem. Phys.* **1985,** *82* (1), 270-283.
93. Couty, M.; Hall, M. B., Basis sets for transition metals: Optimized outerp functions. *J. Comp. Chem.* **1996,** *17* (11), 1359-1370.
94. McLean, A. D.; Chandler, G. S., Contracted Gaussian basis sets for molecular calculations. I. Second row atoms, Z=11–18. *J. Chem. Phys.* **1980,** *72* (10), 5639-5648.
95. Krishnan, R.; Binkley, J. S.; Seeger, R.; Pople, J. A., Self-consistent molecular orbital methods. XX. A basis set for correlated wave functions. *J. Chem. Phys.* **1980,** *72* (1), 650-654.
96. Barone, V.; Cossi, M., Quantum Calculation of Molecular Energies and Energy Gradients in Solution by a Conductor Solvent Model. *The J. Phys. Chem. A* **1998,** *102* (11), 1995-2001.
97. Cossi, M.; Rega, N.; Scalmani, G.; Barone, V., Energies, structures, and electronic properties of molecules in solution with the C-PCM solvation model. *J. Comp. Chem.* **2003,** *24* (6), 669-681.
98. Clark, K. M.; Ziller, J. W.; Heyduk, A. F., Steric Control of Coordination Geometry in Titanium-Imido Complexes of N,N '-bis(arylimino)acenaphthylene Ligands. *Inorg. Chem.* **2010,** *49* (5), 2222-2231.
99. El-Ayaan, U.; Murata, F.; El-Derby, S.; Fukuda, Y., Synthesis, structural and solvent influence studies on solvatochromic mixed-ligand copper(II) complexes with the rigid nitrogen ligand: bis[N-(2,4,6-trimethylphenyl)imino]acenaphthene. *J. Mol. Struc.* **2004,** *692* (1-3), 209-216.
100. Stanciu, C.; Jones, M. E.; Fanwick, P. E.; Abu-Omar, M. M., Multi-electron Activation of Dioxygen on Zirconium(IV) to Give an Unprecedented Bisperoxo Complex. *J. Am. Chem. Soc.* **2007,** *129* (41), 12400-12401.
101. Fedushkin, I. L.; Makarov, V. M.; Sokolov, V. G.; Fukin, G. K.; Maslov, M. O.; Ketkov, S. Y., Compounds of chromium, titanium, and zirconium with different reduced forms of acenaphthene-1,2-diimine. *Russ. Chem. Bull.* **2014,** *63* (4), 870-882.
102. Hessen, B.; Bol, J. E.; Deboer, J. L.; Meetsma, A.; Teuben, J. H., Enediamide Complexes of Hafnium - X-Ray Structure of $[(C_5Me_5)Hf(Pr^iNCHCHNPr^i)(\mu\text{-}H)]_2$. *Chem. Commun.* **1989,** (17), 1276-1277.

103. Nakamura, A.; Mashima, K., 'Supine' or 'prone' ligands: geometric preference of conjugated diene, 1-azadiene, and 1,4-diazadiene ligands on half-metallocene complexes of early transition metals. *J. Organomet. Chem.* **2001,** *621* (1-2), 224-230.
104. Schrempp, D. F.; Schneider, E.; Kaifer, E.; Wadepohl, H.; Himmel, H.-J., Homo- and Heterobinuclear Cu and Pd Complexes with a Bridging Redox-Active Bisguanidino-Substituted Dioxolene Ligand: Electronic Structure and Metal-Ligand Electron-Transfer. *Chem. Eur. J.* **2017,** *23* (48), 11636-11648.
105. Flanagan, J. B.; Margel, S.; Bard, A. J.; Anson, F. C., Electron transfer to and from molecules containing multiple, noninteracting redox centers. Electrochemical oxidation of poly(vinylferrocene). *J. Am. Chem. Soc.* **1978,** *100* (13), 4248-4253.
106. Gagne, R. R.; Ingle, D. M., Intramolecular electron transfer and valence isomerization in mononuclear nickel-macrocyclic ligand complexes: formation of paramagnetic nickel(I)-carbonyl complexes. *J. Am. Chem. Soc.* **1980,** *102* (4), 1444-1446.
107. Gagne, R. R.; Koval, C. A.; Smith, T. J.; Cimolino, M. C., Binuclear complexes of macrocyclic ligands. Electrochemical and spectral properties of homobinuclear CuIICuII, CuIICuI, and CuICuI species including an estimated intramolecular electron transfer rate. *J. Am. Chem. Soc.* **1979,** *101* (16), 4571-4580.
108. D'Alessandro, D. M.; Keene, F. R., A cautionary warning on the use of electrochemical measurements to calculate comproportionation constants for mixed-valence compounds. *Dalton Trans.* **2004,** (23), 3950-3954..
109. Day, P., Mixed-Valency Compounds. *Endeavour* **1970,** *29* (106), 45-49.
110. Robin, M. B.; Day, P., Mixed Valence Chemistry: A Survey and Classification. *Adv. Inorg. Chem. Radiochem.* **1967,** *10*, 247-423.
111. Cao, Z.; Xi, B.; Jodoin, D. S.; Zhang, L.; Cummings, S. P.; Gao, Y.; Tyler, S. F.; Fanwick, P. E.; Crutchley, R. J.; Ren, T., Diruthenium–Polyyn-diyl–Diruthenium Wires: Electronic Coupling in the Long Distance Regime. *J. Am. Chem. Soc.* **2014,** *136* (34), 12174-12183.
112. Kaim, W.; Klein, A.; Glöckle, M., Exploration of Mixed-Valence Chemistry: Inventing New Analogues of the Creutz-Taube Ion. *Acc. Chem. Res.* **2000,** *33* (11), 755-763.
113. Kaim, W.; Sarkar, B., Mixed valency in ruthenium complexes—Coordinative aspects. *Coord. Chem. Rev.* **2007,** *251* (3-4), 584-594.
114. Ying, J.-W.; Liu, I. P.-C.; Xi, B.; Song, Y.; Campana, C.; Zuo, J.-L.; Ren, T., Linear Trimer of Diruthenium Linked by Butadiyn-Diyl Units: A Unique Electronic Wire. *Angew. Chem., Int. Ed.* **2010,** *49* (5), 954-957.
115. Crutchley, R. J., Intervalence Charge Transfer and Electron Exchange Studies of Dinuclear Ruthenium Complexes. *Adv. Inorg. Chem.* **1994,** *41*, 273-325.
116. Cotton, S. A., Titanium, zirconium, hafnium. *annu. rep. prog. chem., sect. a: inorg. chem.* **2012,** *108*, 146-155.
117. Klein, R. A.; Elsevier, C. J.; Hartl, F., Redox Properties of Zerovalent Palladium Complexes Containing α-Diimine andp-Quinone Ligands. *Organometallics* **1997,** *16* (6), 1284-1291.
118. Fryzuk, M. D.; Mylvaganam, M.; Zaworotko, M. J.; Macgillivray, L. R., Synthesis of Mononuclear Paramagnetic Zirconium(III) Derivatives. *J. Am. Chem. Soc.* **1993,** *115* (22), 10360-10361.
119. Grant, L. N.; Miehlich, M. E.; Meyer, K.; Mindiola, D. J., Arrested disproportionation in trivalent, mononuclear, and non-metallocene complexes of Zr(III) and Hf(III). *Chem. Commun.* **2018,** *54* (16), 2052-2055.
120. Wielstra, Y.; Gambarotta, S.; Chiang, M. Y., The elusive zirconium(III). *Recl. Trav. Chim. Pay-B* **2010,** *108* (1), 1-6.
121. Lancaster, S. J., Complexes of Zirconium and Hafnium in Oxidation State iii. In *Comprehensive Organometallic Chemistry III*, 2007; pp 741-757.
122. Cotton, S. A.; Hart, F. A., Zirconium and Hafnium. In *The Heavy Transition Elements*, 1975; pp 3-14.
123. Lappert, M. F.; Pickett, C. J.; Riley, P. I.; Yarrow, P. I. W., Metallocene derivatives of early transition metals. Part 2. Substituted cyclopentadienyl Group 4A dichloro-metallocene complexes $[M(\eta\text{-}C5H4R)_2Cl_2]$(M = Zr or Hf; R = Me, Et, Pr^i, Bu^t, or $SiMe_3$), their mono- and di-alkyl derivatives $[M(\eta\text{-}C_5H_4R)_2R'X]$(X = Cl or R′; R′= CH_2SiMe_3 or CH_2CMe_3), and their d^1 reduction products. *J. Chem. Soc., Dalton Trans.* **1981,** (3), 805-813.
124. Parry, E. P.; Osteryoung, R. A., Evaluation of Analytical Pulse Polarography. *Anal. Chem.* **1965,** *37* (13), 1634-1637.
125. Sutton, J. E.; Taube, H., Metal to Metal Interactions in Weakly Coupled Mixed-Valence Complexes Based on Ruthenium Ammines. *Inorg. Chem.* **1981,** *20* (10), 3126-3134.
126. Wang, X.-Y.; Avendaño, C.; Dunbar, K. R., Molecular magnetic materials based on 4*d* and 5*d* transition metals. *Chem. Soc. Rev.***2011,** *40* (6).
127. Connelly, N. G.; Geiger, W. E., Chemical redox agents for organometallic chemistry. *Chem. Rev.* **1996,** *96* (2), 877-910.
128. Chalk, S. J., isosbestic point. In *IUPAC Compendium of Chemical Terminology*, 2007; p 359.
129. Morrey, J. R., Isosbestic Points in Absorbance Spectra. *J. Phys. Chem.* **1963,** *67* (7), 1569-1569.
130. Cohen, M. D.; Fischer, E., 588. Isosbestic points. *J. Chem. Soc.* **1962**, 3044-3052.
131. Biagini, P.; Calderazzo, F.; Pampaloni, G.; Zanazzi, P. F., Reactions of Group-IVB (Group 4) Metal (Ti, Zr, Hf) Derivatives with Biscyclopentadienylcobalt(II) and Its Permethylated Analog - Effect of Halide, Solvent and Metal. *Gazz. Chim. Ital.* **1987,** *117* (1), 27-37.
132. Rohm, H. W.; Köckerling, M., New Double Salts with Boron-Centered Zirconium Clusters: Syntheses and Structures of $Cs[ZrCl_5]\cdot Cs_2[(Zr_6B)X_{15}]$ (X = Cl or Cl+I), and Anion Distribution in the Mixed Halide Phase. *Z. Anorg. Allg. Chem.* **2003,** *629* (1213), 2356-2362.
133. Weil, J. A.; Bolton, J.R., Relaxation Times, Linewidths and Spin Kinetic Phenomena. In *Electron Paramagnetic Resonance*, Weil, J. A., Bolton, J.R., Eds. John Wiley & Sons: 2006; pp 301-356.
134. Claxton, T. A.; Oakes, J., "Variable" hyperfine coupling constants. *Chem. Phys. Lett.* **1967,** *1* (5), 189-190.
135. Claxton, T. A.; Oakes, J.; Symons, M. C. R., Origin of Linewidth Alternation in Semiquinone–Alkali Metal Systems. *Nature* **1967,** *216* (5118), 914-915.
136. Poole, C. P. F., H.A., Lineshapes in Electron Spin Resonance. *Bull. Magn. Reson.* **1979,** *1* (4), 162-194.
137. Röder, J. C.; Meyer, F.; Hyla-Kryspin, I.; Winter, R. F.; Kaifer, E., Electronic Coupling in a Highly Preorganized Bimetallic Complex Comprising Pyrazolate-Bridged $CpMn(CO)_2$ Moieties. *Chem. Eur. J.* **2003,** *9* (11), 2636-2648.
138. The IVCT bands identified by TD-DFT for $\mathbf{2}^-$ and $\mathbf{3}^-$ are consistent the NIR spectra; however, there is some deviation in the for $\mathbf{1}^-$. Only two bands, at 1742 nm and 981 nm, were by TD-DFT for this complex, whilst the experimentally observed IVCT band at 1222 nm appears as a dark transition. We suspect that this deviation suggests more complex behavior in $\mathbf{1}^-$ that is not accounted for by our model.
139. Xu, G.-L.; Crutchley, R. J.; DeRosa, M. C.; Pan, Q.-J.; Zhang, H.-X.; Wang, X.; Ren, T., Strong Electronic Couplings between Ferrocenyl Centers Mediated by Bis-Ethynyl/Butadiynyl Diruthenium Bridges. *J. Am. Chem. Soc.* **2005,** *127* (38), 13354-13363.

140. Launay, J. P., Mixed-Valent Compounds and their Properties - Recent Developments. *Eur. J. Inorg. Chem.* **2020,** *2020* (4), 329-341.
141. Demadis, K. D.; Hartshorn, C. M.; Meyer, T. J., The localized-to-delocalized transition in mixed-valence chemistry. *Chem. Rev.* **2001,** *101* (9), 2655-2685.
142. D'Alessandro, D. M.; Keene, F. R., Current trends and future challenges in the experimental, theoretical and computational analysis of intervalence charge transfer (IVCT) transitions. *Chem. Soc. Rev.***2006,** *35* (5), 424-440.
143. Hush, N. S., Homogeneous and Heterogeneous Optical and Thermal Electron Transfer. *Electrochim. Acta* **1968,** *13* (5), 1005-1023.
144. Hush, N. S., Distance Dependence of Electron-Transfer Rates. *Coord. Chem. Rev.* **1985,** *64*, 135-157.
145. Brunschwig, B. S.; Creutz, C.; Sutin, N., Optical transitions of symmetrical mixed-valence systems in the Class II-III transition regime. *Chem. Soc. Rev.* **2002,** *31* (3), 168-184.
146. Rhoda, H. M.; Chanawanno, K.; King, A. J.; Zatsikha, Y. V.; Ziegler, C. J.; Nemykin, V. N., Unusually Strong Long-Distance Metal-Metal Coupling in Bis(ferrocene)-Containing BOPHY: An Introduction to Organometallic BOPHYs. *Chem. Eur. J.* **2015,** *21* (50), 18043-18046.
147. Patoux, C.; Coudret, C.; Launay, J. P.; Joachim, C.; Gourdon, A., Topological effects on intramolecular electron transfer via quantum interference. *Inorg. Chem.* **1997,** *36* (22), 5037-5049.
148. Paddon-Row, M. N., Investigating long-range electron-transfer processes with rigid, covalently linked donor-(norbornylogous bridge)-acceptor systems. *Acc. Chem. Res.* **1994,** *27* (1), 18-25.
149. Rosokha, S. V.; Kochi, J. K., Fresh Look at Electron-Transfer Mechanisms via the Donor/Acceptor Bindings in the Critical Encounter Complex. *Acc. Chem. Res.* **2008,** *41* (5), 641-653.

Authors are required to submit a graphic entry for the Table of Contents (TOC) that, in conjunction with the manuscript title, should give the reader a representative idea of one of the following: A key structure, reaction, equation, concept, or theorem, etc., that is discussed in the manuscript. Consult the journal's Instructions for Authors for TOC graphic specifications.

Insert Table of Contents artwork here